2020
doi:10.1017/S1431927616010941
Microsc. Microanal. 22 (Suppl 3), 2016

"Colossal" Interstitial Supersaturation in Delta Ferrite in 17-7 PH Stainless Steels After Low-temperature Nitridation

D. Wang, H. Kahn, F. Ernst, and A.H. Heuer

Department of Materials Science and Engineering, Case Western Reserve University, Cleveland, OH, USA

A carbon-induced spinodal decomposition of delta ferrite to nanometer-scale Cr-rich and Fe-rich alpha ferrite phases was observed in the weak-contrast regions in high-resolution scanning TEM (STEM) [1]. In addition, an extremely high dislocation density was observed in the decomposed regions, which is consistent with the hypothesis that carbon segregation to dislocation cores effectively delays carbide precipitation and makes possible the "colossal" carbon supersaturation.

Low-temperature gas-phase nitridation has been studied in interstitially-hardened 17-7 precipitation-hardening stainless steel. After nitridation, conventional transmission electron microscopy reveals that delta ferrite grains in such alloys show a uniformly weak diffraction contrast. Weak-contrast ferrite grains can be observed after nitridation at 713 K with a nitriding activity of 7400, as shown in Fig. 1. In the cross section of the nitrided sample, two ferrite grains close to the free surface (which is on the right) show weak contrast. The ferrite grain that is deeper in the case (arrowed in Fig. 1) shows weak contrast in its top half, but regular diffraction contrast in its bottom half. This illustrates that during the low-temperature nitridation, ferrite grains can transform into a "phase" showing weak contrast directly, without the transitional, plate-containing morphology we observed in the case of low-temperature carburization of the same alloy [1].

A diffraction pattern acquired from a ferrite nitrided at 713 K along a $<011>_{BCC}$ zone axis is shown in Fig. 2a. There are diffuse streaks along a $[001]_{BCC}$ direction towards smaller reciprocal lattice spacings, similar to those of carburized ferrite in this steel [1]. Surprisingly, there is no significant tetragonality in these weak-contrast ferrite grains. In addition, there is an additional set of reflections in the $<011>_{BCC}$ pattern, which indicates a second phase possessing a cubic (rocksalt) structure, MN (with M being a combination of Fe, Cr, Ni, and Al), and forming the Bain orientation relationship with the matrix [2].

Figures 2c and 2d show diffraction patterns acquired from the partially nitrided (arrowed) ferrite grain shown in Fig. 1a. Both patterns show extra reflections due to NiAl precipitates (the weak reflections between BCC matrix reflections). Comparing the two diffraction patterns recorded from the weak-contrast (top) and original (bottom) portions of the grain, in the absence of nitride reflections, all reflections (including ferrite matrix and NiAl reflections) are present. Except for the diffraction pattern acquired from the weak-contrast region (Fig. 2d), there are signs of diffuse streaks along $[001]_{BCC}$ directions towards smaller reciprocal spacings (reflections are elongated rather than circular), suggesting the weak-contrast appearance is related to a lattice distortion (local expansion) in the ferrite, and that nitride formation is not necessary for the weak-contrast appearance.

Strain analysis was performed on the same partially transformed delta ferrite grain. Figure 3b is a virtual bright-field image of the image shown in Fig. 3a; the grain in red is where the strain maps were acquired. Figure 3c shows the reference diffraction pattern used in the strain analysis. The reference diffraction pattern was acquired from the original ferrite region; the corresponding strain at the reference point is set to be 0. The lines in Figs. 3b and 3c indicate the directions of the strain analysis – [001] BCC

in the *x* direction. Figures 3d and 3e are the strain maps along the *x* and *y* directions with respect to the [001]BCC direction. The map shows that the strains within the transforming ferrite grain can be as large as 2.5%. Since this strain is much higher than the expected yield strain, plastic deformation would be expected within the grain. Further, the observed strain could explain the streak formation in Fig. 2d, i.e. local deformation was induced by the nitridation process. The compressive strain in the *y* direction of the grain generally follows the diffusion direction of nitrogen in the sample. The strain map also suggests ≈ 1.5 % deformation threshold for the weak-contrast transformation.

Chemical analysis shows that the weak-contrast ferrite grains contain an enormous interstitial nitrogen supersaturation (> 20 at.%). Such weak diffraction contrast is attributed to a nanometer-scale nitridation-induced spinodal decomposition of delta ferrite grains.

References:
[1] D. Wang, *et al*, Acta Mater. **86** (2015), p. 193.
[2] H. Dong, M. Esfandiari, X.Y. Li, Surf. Coat. Technol. **202** (2008), p. 2969.

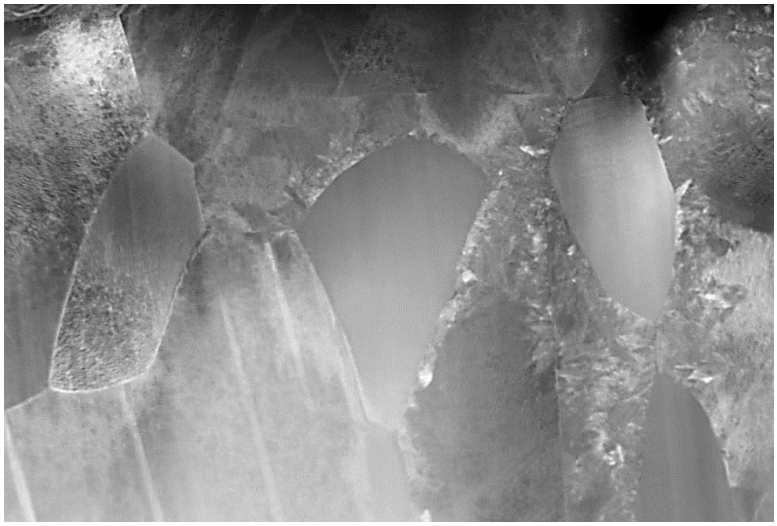

Figure 1. STEM images of cross sections of nitrided 17-7 PH stainless steel. The original alloy surface is ≈ 6 μm to the right (nitridation at 713 K, nitrogen activity of 7400). Grains 1 and 2 show the weak contrast, while only the top half of grain 3 shows this contrast.

https://doi.org/10.1017/S1431927616010941 Published online by Cambridge University Press

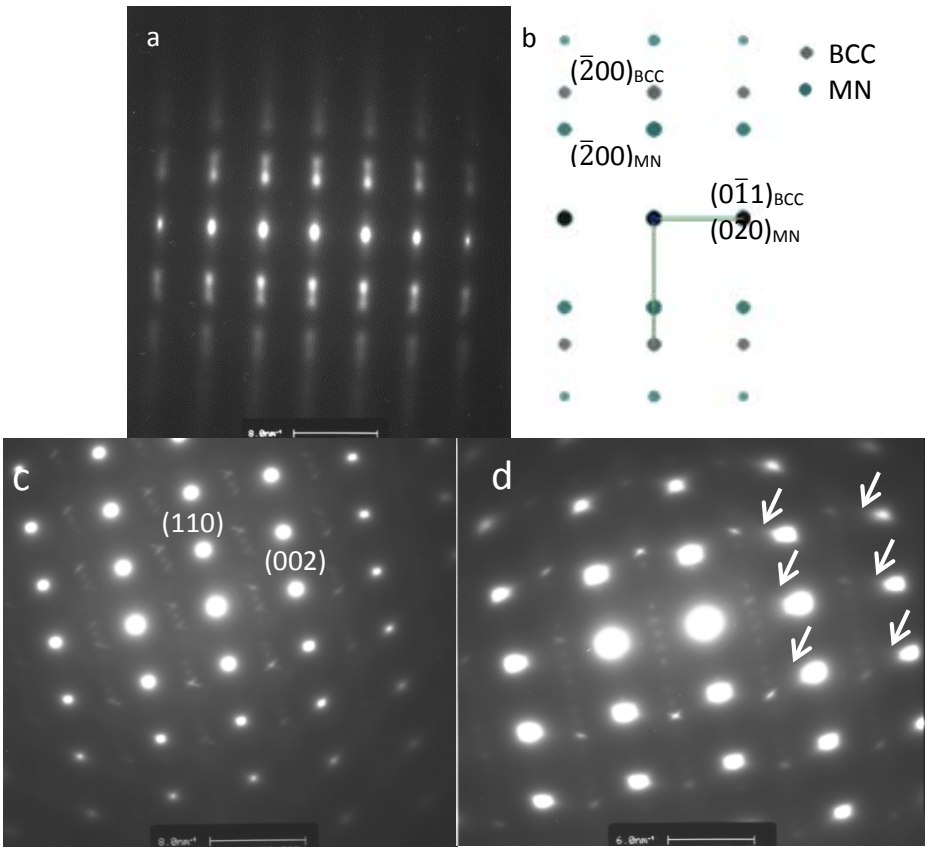

Fig. 2 (a) Diffraction pattern acquired from a $<011>_{BCC}$ zone axis of a nitrided weak-contrast delta ferrite grain. (b) Simulation of the BCC ferrite and the rocksalt-structured nitride obeying the Bain orientation relation. (c) and (d) Diffraction patterns acquired from the arrowed ferrite grain shown in Fig. 1. (c) is from the lower portion of the grain (the original structure) and (d) is from the top, weak-contrast region. Signs of early-stage streaks are arrowed in (d).

https://doi.org/10.1017/S1431927616010941 Published online by Cambridge University Press

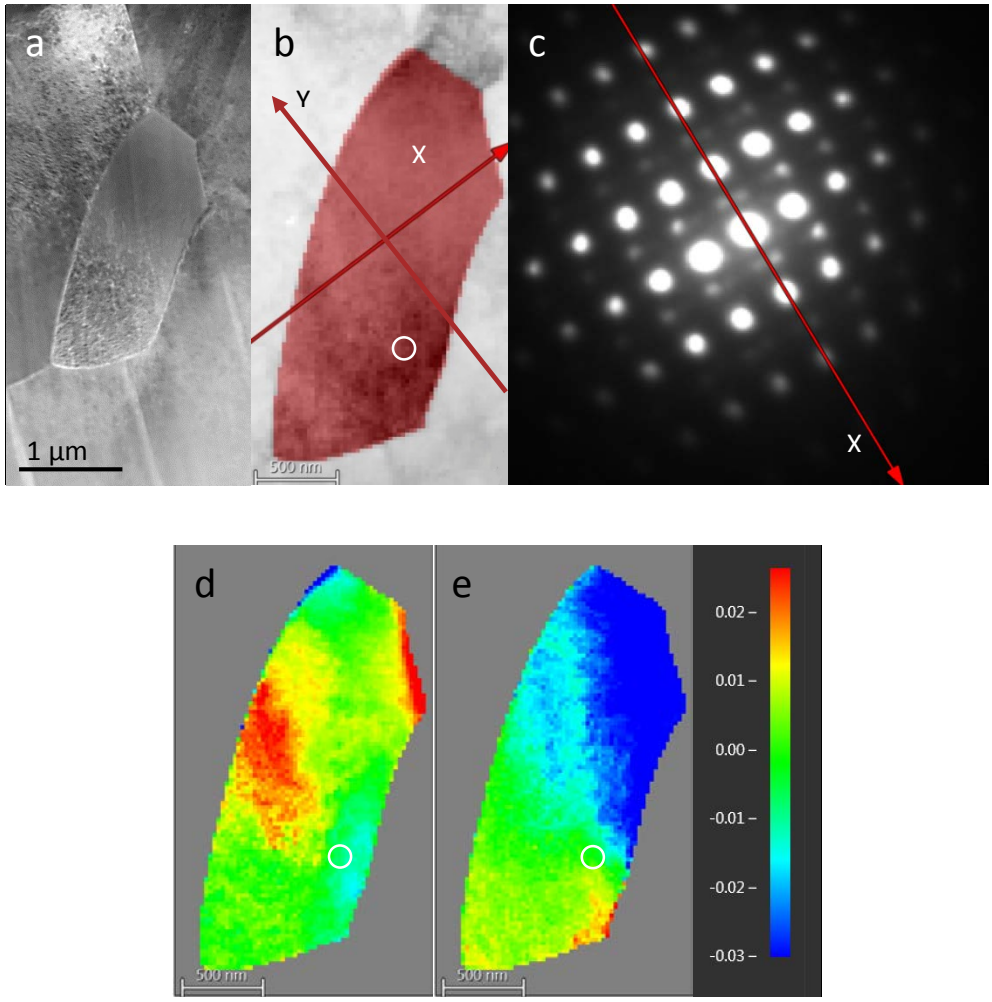

Fig. 3 Strain anlysis of the arrowed delta ferrite grain in Fig. 1a. (a) STEM image and (b) virtual bright-field image. The grain in red is where the strain analysis was acquired. The arrows indicate the *x* and *y* directions of the strain analysis in real space. (c) Reference diffraction pattern showing the *x* direction ([001]$_{BCC}$) of strain analysis in reciprocal space. (d) and (e) are strain maps along the *x* and *y* directions, respectively. The circles in (b), (d), and (e) indicate where the reference diffraction pattern was acquired.

https://doi.org/10.1017/S1431927616010941 Published online by Cambridge University Press